

Mechanisms of Deformation of Silicon Nitride and Silicon Carbide at High Temperatures

Sheldon M. Wiederhorn,* B. J. Hockey and J. D. French

National Institute of Standards and Technology, Gaithersburg, MD 20899, USA

Abstract

This paper compares the relative merits of liquid-phase sintered β -Si₃N₄ with sintered α -SiC for high-temperature applications. These materials represent two extremes of ceramic microstructure: liquid-phase sintered β -Si₃N₄ contains grains that are coated by a second phase, whereas sintered α -SiC contains grains that are in direct crystalline contact. As will be shown, the mechanical behavior of the two materials differs substantially. At temperatures up to 1500 °C, sintered α -SiC is a creep-resistant solid. At room temperature, however, it is brittle, $K_{Ic} = (2-4)$ MPa·m^{1/2}, and has a low bending strength, $\sigma_b = (400-500)$ MPa. By contrast, liquid-phase sintered β -Si₃N₄ is not as creep resistant since it contains a residual sintering aid at its grain boundaries that deforms at a lower temperature than the silicon nitride grains. Hence, its temperature capability is less than that of sintered α -SiC. Silicon nitride is, however, tougher, $K_{Ic} = (6-8)$ MPa·m^{1/2}, and stronger, $\sigma_b = (700-1000)$ MPa, than sintered α -SiC. Deformation of liquid-phase sintered β -Si₃N₄, and other ceramics with a second phase at the grain boundaries, depends on the refractoriness of that phase, the more refractory the phase, the more resistant the material is to creep. Experimental results on β -Si₃N₄ suggest that toughness decreases as creep resistance increases; hence, a trade-off must be made between creep resistance and material toughness to achieve an optimal high temperature microstructure. © 1999 Elsevier Science Ltd. All rights reserved.

Keywords: microstructure-final, creep, mechanical properties, strength, toughness, SiC, Si₃N₄.

1 Introduction

An understanding of the creep behavior of ceramic materials is necessary in order to determine lifetime limits in applications where resistance to high temperatures is needed. Silicon carbide and silicon nitride are two commercial materials that are used in high temperature structural applications. Silicon carbide is used as muffle furnace linings, kiln furniture and as parts in high temperature heat exchangers.^{1,2} Silicon nitride was specifically developed for use in gas turbines to satisfy the needs for higher operating temperatures and greater efficiencies in automotive,³ space⁴ and electric power generating applications.⁵⁻⁷ Commercial grades of this material are currently being evaluated in experimental gas turbines.⁶ Although the creep behavior of both materials has been studied extensively during the past 10 years, no recent comparison of their relative merits for high temperature applications has been made. A review of the subject by Davis and Carter,⁸ covers publications before 1985 and so does not review tensile creep data obtained since then on modern grades of silicon nitride or silicon carbide. The recent review article by Raj on structural ceramics for service near 2000 °C also does not cover the creep behavior of these materials.⁹ In this paper, we discuss and compare the creep resistance of silicon nitrides and silicon carbides intended for high temperature applications. We first discuss the microstructure of these materials and then compare their creep behavior. Finally, theories of creep behavior are discussed and methods of improving creep behavior are suggested.

Current grades of silicon carbide and silicon nitride can be idealized by one of two types of microstructures. In the first, grains are in direct crystalline contact with one another, being separated by grain boundaries that are free of a second phase. Creep then occurs by deformation of the grains themselves, by dislocation motion, or by

*To whom correspondence should be addressed.

classical diffusion processes, in which bulk or grain boundary diffusion through or around the grains, or near dislocations controls the rate of creep.^{10–12} This type of microstructure can be made by sintering,^{13–15} by vapor deposition,^{11,16} or by direct reaction as in reaction-bonded silicon nitride.^{10,17} The second type of microstructure is made by liquid-phase sintering and has grains that are covered by a second phase.^{18–20} True grain boundaries do not exist in these materials. The intergranular phase softens at lower temperatures than the more refractory silicon nitride or silicon carbide grains, and creep is controlled by deformation of that phase. In the discussion that follows, we refer to grains that are covered with a second phase as “wetted” grain boundaries; boundaries that are free of a second phase are called “dry” or “unwetted” grain boundaries.

Of the commercial grades of silicon nitride and silicon carbide that fit into these two categories, two will be the primary subject of discussion in this paper: sintered α -SiC, a fully dense material with “dry” grain boundaries, and liquid-phase sintered β -Si₃N₄, a material with fully “wetted” grain boundaries. We also discuss reaction-bonded silicon carbide, which contain “dry” boundaries between directly bonded grains of silicon carbide. The creep behavior of reaction-bonded silicon carbide, however, depends on the amount of silicon within the material. With small amounts of silicon, creep is controlled by the grains that are directly bonded and deformation occurs by deformation of the silicon carbide grains themselves, as in other grades of silicon carbide with “dry” boundaries. With large amounts of silicon, however, contacts between the grains are easily broken. Then, creep is controlled by deformation of the silicon phase and the behavior of the material is similar to that of materials with wetted boundaries.

2 Microstructures of α -SiC and β -Si₃N₄

2.1 α -SiC

The microstructure of sintered silicon carbide depends on the method of manufacture. Because silicon carbide is a covalent material, bulk diffusion through the grains is too slow to achieve full density without the use of sintering aids. Boron and carbon^{2,13–15} are usually used for this purpose. The carbon removes SiO₂ from the surface of the grains, converting it to SiC.¹⁵ The role of the sintering aids is not fully understood, although they are believed to affect grain boundary and surface energies and to enhance diffusion rates.¹⁴ A sintering temperature of 2150 °C for about 30 min is required for full density.² Although large pieces of

silicon carbide can be made by this technique, they are brittle, $K_{Ic} \approx 3 \text{ MPa} \cdot \text{m}^{-1/2}$ and have a low strength, $\sigma_b = (400–500) \text{ MPa}$.¹⁴ The microstructure of a grade of α -SiC (Hexoloy, Carborundum, Niagara Falls, NY)* made by this method is shown in Fig. 1(a). As can be seen the material contains blocky grains of α -SiC approximately 2–5 μm in diameter. Residual graphite inclusions occur at multi-grain junctions. Despite the use of carbon to reduce SiO₂ at the grain boundaries, some residual glass is still found at triple junctions, Fig. 1(b). Most of the boundaries are, however, free of glass.

High density, impermeable silicon carbides can be made at a lower temperature by partially sintering the SiC powder compact, and then infiltrating it with molten silicon.^{14,21,22} The volume fraction of silicon carbide of such microstructures

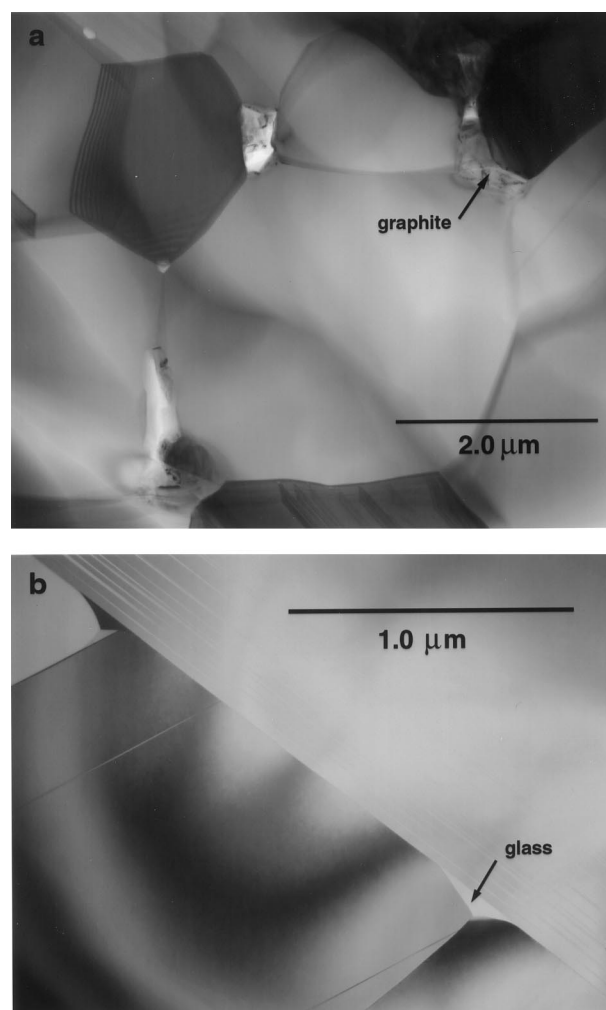


Fig. 1. Transmission electron micrographs of Hexoloy, a grade of sintered α -SiC made by Carborundum: (a) blocky grains with graphite at multi-grain junctions; (b) grain boundary wetted by glass.

*The use of commercial designations is for purpose of identification only. It does not imply endorsement by the National Institute of Standards and Technology.

ranges from about 67 to about 92%. Carbon is added to the SiC compact to remove SiO₂ from the surface of the grains; boron is not used. The silicon reacts with the carbon to produce more silicon carbide, which grows on the SiC grains.¹⁸

The microstructures of three materials of this type are shown in Fig. 2. These include NT230 (St. Gobain/Norton Industrial Ceramics Corp., 8% volume fraction Si), SCRB210 (Coors, Golden, CO, 18% volume fraction Si), and KX01 (Carborundum, Niagara Falls, NY, 33% volume fraction Si). To increase the volume fraction of SiC in the solid, the SCRB210 was made of a mixture of 2–4 μm SiC and 10–30 μm SiC. Both the silicon and the silicon carbide structures are interconnected for all three materials. Transmission electron microscopy studies on KX01,¹⁸ SCRB210²³ and other grades of reaction bonded silicon carbide¹⁰ show that the boundaries between silicon carbide grains are unwetted. Because of the small area of contact between the silicon carbide grains in KX01 and SCRB210, however, contacts between the grains are tenuous,¹⁸ so that during deformation the SiC grain boundaries fracture, and the main resistance to creep occurs by deformation of the silicon.¹⁸ Thus, though KX01 and SCRB210 are made by reaction bonding, they behave more like materials with “wetted” boundaries when deformed at high temperatures. By contrast, the silicon phase in NT230 is restricted to channels running through the solid.²⁴ Most of the SiC grains are in direct contact and are separated by “dry” grain boundaries, Fig. 2(c). They are not wetted by the molten silicon during the process of manufacture. Deformation of this material, therefore, requires deformation of the grains themselves, rather than the silicon at the grain boundaries.

2.2 Si₃N₄

Most commercial grades of silicon nitride are made with sintering aids that promote liquid-phase sintering at temperatures of 1825–2080°C.¹⁷ High pressure nitrogen, 1–8 MPa, is used to prevent decomposition of silicon nitride at these temperatures.^{25,26} Because of the way it is made, the microstructure of the silicon nitride is very different from that of sintered silicon carbide. As can be seen in Fig. 3, each grain of silicon nitride is surrounded by a silicate phase that results from a reaction between the sintering aid and residual silica on the surface of the silicon nitride powder. The grains of silicon nitride are separated by a ~0.5 nm to ~1 nm layer of amorphous silicate, Fig. 4(a), whose thickness depends primarily on the chemical composition of the sintering aid.^{27,28} At temperatures between 1200 and 1400°C the silicate phase in the multi-grain junctions partially devitrifies, forming a variety of crystalline phases.^{28–30} Devitrification is never total, because a thin layer of an amorphous phase, 2–3 nm thick, Fig. 4(b), always separates the crystalline silicate phase from the silicon nitride grain.^{27,28} The thickness of the amorphous phases can be rationalized by the model of interlayer thicknesses proposed by Clarke.²⁷ Examples of the sintering aids used and the crystalline phases that form in some modern commercial grades of silicon nitride are given in Table 1.

The mechanical properties of the silicon nitride at high temperatures depend on the amount and composition of the sintering aid used to process it.³¹ Because the sintering aid softens at a lower temperature than the silicon nitride grains, a refractory sintering aid is required for high-temperature applications. Rare earth oxides such as

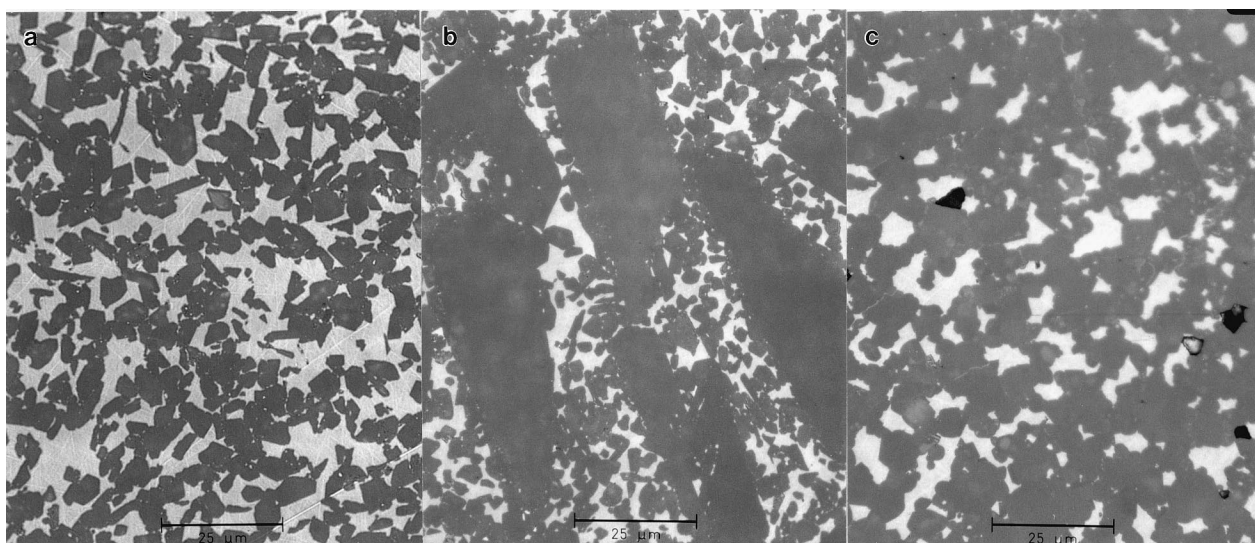


Fig. 2. Photomicrographs of the microstructure of reaction-bonded SiC: (a) KX01 (carborundum, Niagara Falls, NY, 33% volume fraction Si); (b) SCRB210 (Coors, Golden, CO, 18% volume fraction Si); (c) NT230 (St. Gobain/Norton Industrial Ceramics Corp., 8% volume fraction Si).

yttrium oxide, which form high temperature eutectics are normally used as sintering aids,²⁸ also see Table 1. For lower temperature applications, toughness and strength are enhanced by *in situ*

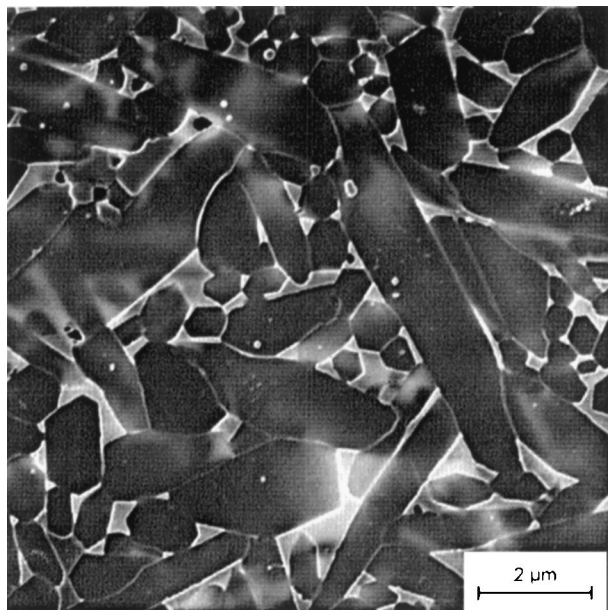


Fig. 3. Scanning electron micrograph of a plasma etched surface of silicon nitride: SN88 NGK Insulator, Inc., Nagoya, Japan; The darker phase is the silicon nitride and the lighter phase is the residual sintering aid.

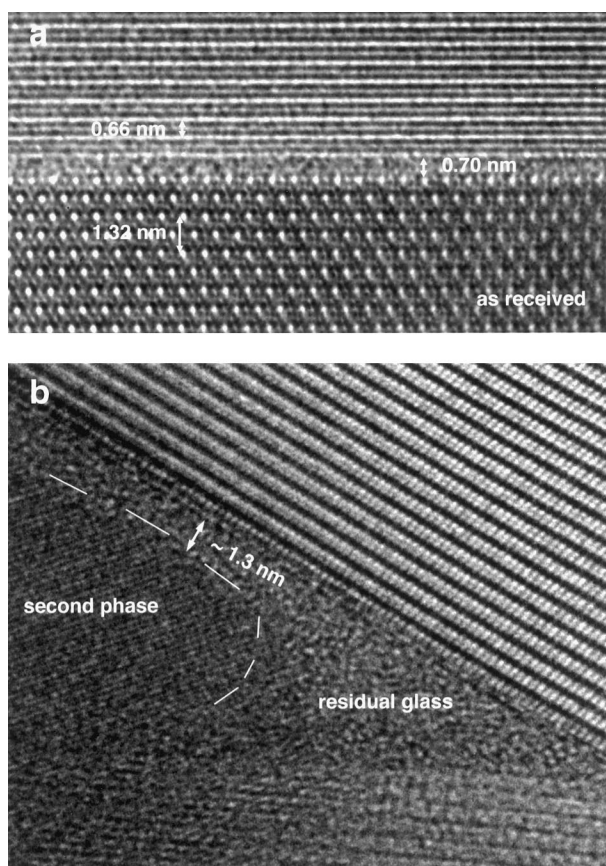


Fig. 4. Transmission electron micrographs of silicon nitride, SN88, showing residual sintering aid: (a) thin layer of silicate phase separating two grains of silicon nitride; (b) multi-grain junction showing the thicker boundary separating the silicon nitride grains and the crystalline silicate phase.

toughening, in which sintering aids such as Al_2O_3 , MgO , and CaO cause the grains of silicon nitride to grow in length to increase their aspect ratio.^{32–35} High toughness is achieved by debonding along the silicon nitride grains during fracture, thus promoting bridging across the propagating crack.^{36,37} Commercial grades of silicon nitride made in this way have critical stress intensity factors as high as $K_{\text{Ic}} = 8 \text{ MPa} \cdot \text{m}^{1/2}$ ^{38,39} and bending strengths, σ_b , as high as 1000 MPa.^{39,40}

3 Creep Behavior

3.1 Silicon carbide

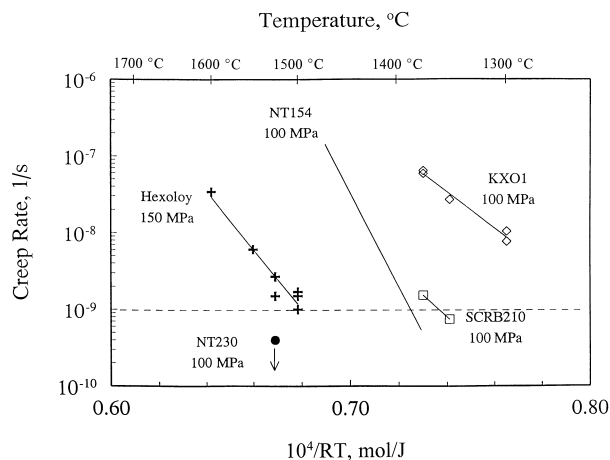
Figure 5 compares the tensile creep behavior of Hexoloy with that of silicon nitride, NT154 [41]* and three grades of reaction-bonded silicon carbide. Creep data from the NT154 are included in the figure because its creep resistance is higher than most other commercial grades of silicon nitride.⁴² A dashed line at $1 \times 10^{-9} \text{ s}^{-1}$ is plotted on the figure as an index of long term lifetime. If a failure strain of 1% is assumed, then $1 \times 10^{-9} \text{ s}^{-1}$ gives a lifetime of about 4 months. The most creep resistant material in Fig. 5, NT230, crept too slowly, $< 4 \times 10^{-10} \text{ s}^{-1}$, at 1525°C and 100 MPa²⁴ to be measured on the equipment used for the study. If the NT230 has about the same activation energy for creep as the Hexoloy, the highest temperature of use for a 4 month lifetime is $> 1550^\circ\text{C}$. Of the remaining four materials, the Hexoloy (sintered α -SiC) is easily the most creep resistant material and can be used at temperatures up to 1500°C. The NT154 is the next most creep resistant material being able to sustain 100 MPa at temperatures up to 1390°C. By contrast, the SCRB210 and the KX01 exhibited the poorest creep behavior, being capable of a sustained tensile stress of 100 MPa at temperatures of only 1360 and 1220°C, respectively.

Figure 6 compares the tensile and compressive creep of Hexoloy¹² with the compressive creep behavior of several grades of silicon carbide. The NC430 (St. Gobain/Norton Industrial Ceramics Corp.),¹⁰ is a grade of reaction-bonded silicon carbide with a volume fraction of about 11% silicon. The SiC A was made by hot-pressing without sintering aid.⁴³ The SiC B is an unnamed commercial grade of silicon carbide containing 1% volume fraction boron and less than 2000 ppm other impurities.⁴³ The compressive creep data on Hexoloy was stress corrected from 179 MPa, reported

*For each figure in which data was collected at the National Institute of Standards and Technology, the relative standard uncertainty is presented in the caption. This parameter is the standard deviation of the fit for each curve.

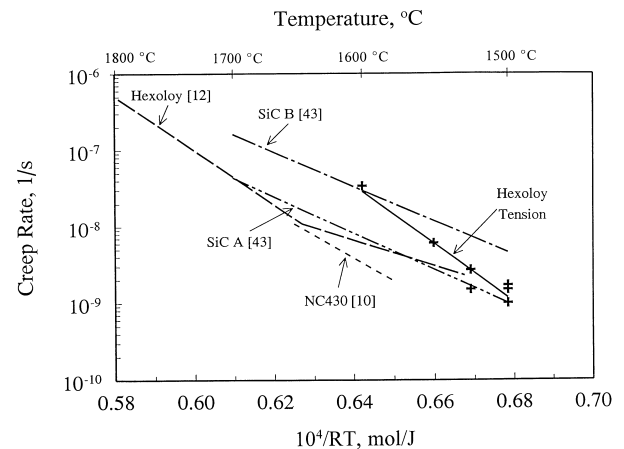
Table 1. Composition and phases in commercial grades of silicon nitride, as determined by transmission electron microscopy analyses

Material	Sintering aid	Phases crystallizing in the residual glass
NT-154	Y ₂ O ₃	α -Y ₂ Si ₂ O ₇ , Y ₅ (SiO ₄) ₃ N {H-Phase}
PY-6	Y ₂ O ₃	α -Y ₂ Si ₂ O ₇ , Y ₅ (SiO ₄) ₃ N {H-Phase}
AY-6	Y ₂ O ₃ , Al ₂ O ₃	δ -Y ₂ SiO ₇ , Y ₅ (SiO ₄) ₃ N {H-Phase}
GN-10	SrO, CaO, Y ₂ O ₃	(Y,Sr,Ca) ₄ Si ₂ O ₇ N ₂ {J-Phase}, (Y,Sr,Ca) ₅ (SiO ₄) ₃ N {H-Phase}
SN-88	Y ₂ O ₃ , Yb ₂ O ₃	(Yb,Y) ₂ Si ₂ O ₇ , (Y,Yb) ₅ (SiO ₄) ₃ N {H-Phase}
AS-800	Y ₂ O ₃ , La ₂ O ₃ , SrO	(La,Y,Sr) ₅ (SiO ₄) ₃ N {H-Phase}, (La,Y) ₂ Si ₂ O ₇

**Fig. 5.** A comparison of the tensile creep behavior of various grades of silicon carbide: Hexoloy; NT230; SCRB210 and KXO1.²⁴ Silicon nitride, NT154, is also included in the figure to compare the reaction sintered silicon carbide with liquid-phase sintered silicon nitride.⁴¹ The relative standard uncertainty of the Hexoloy and KXO1 data was approximately 0.15.

in,¹⁰ to 150 MPa using a stress exponent of 1.6. All of the materials shown in Fig. 6 have been examined by transmission electron microscopy. None had grain boundaries wetted by a silicate phase, which explains their excellent creep resistance.

A comparison of the creep resistance of Hexoloy tested in compression and tension shows that the apparent activation energy in tension, (885 ± 106) kJ mol⁻¹, falls within the range $(801\text{--}914)$ kJ mol⁻¹ reported for the compressive creep of this material at temperatures above 1647°C.¹² This range of activation energies has been attributed to lattice diffusion.¹² The fact that similar values are obtained for the activation energy for creep in tension and compression may indicate that creep in tension is also controlled by lattice diffusion. The results shown in Fig 6 also suggest that Hexoloy is more creep resistant in compression than in tension. However, since measurements were made at different laboratories and on different billets of this material, the available creep data is not sufficient to prove this assumption. Differences in experimental technique at the two laboratories, and lot-to-lot variability in impurity and sintering aid content may also play a role in explaining the results. Further experimentation on sintered silicon carbide

**Fig. 6.** A comparison of the tensile and compressive creep of Hexoloy with the compressive creep of NC430 and two other grades of silicon carbide, SiC A and SiC B. The NC430 (St. Gobain/Norton Industrial Ceramics Corp.) is a grade of reaction-bonded silicon carbide with a volume fraction of silicon¹⁰ of 11%. SiC A is an experimental grade of hot pressed silicon carbide⁴³; SiC B is an unnamed commercial grade of sintered silicon carbide. The apparent activation energy for the Hexoloy data is approximately 885 ± 106 kJ mol⁻¹. The relative standard uncertainty of the Hexoloy data was approximately 0.15.

will be needed both to clarify the creep mechanism and to support the data showing that creep in tension occurs more easily than creep in compression.

Experimental evidence is strong, however, that other grades of silicon carbide exhibit differences in tensile and compressive creep behavior. As shown in Fig. 7, the creep rate of SCRB210 and KXO1 in tension is about 100 times that measured in compression for both materials. Lot-to-lot variability as a cause for the difference in creep behavior was ruled out by using the same billet of material for the tensile and compressive creep tests. Cavities formed in both materials during tensile creep,^{18,44–46} but not during compressive creep.⁴⁶ Furthermore, the volume fraction of cavities in KXO1 is approximately equal to the total creep strain,^{45–47} Fig. 8, suggesting a close relationship between tensile creep and the process of cavitation. Therefore, we believe the difference in creep behavior in tension and compression is a consequence of the cavity formation. As will be shown below, this type of behavior is also observed in silicon nitride.

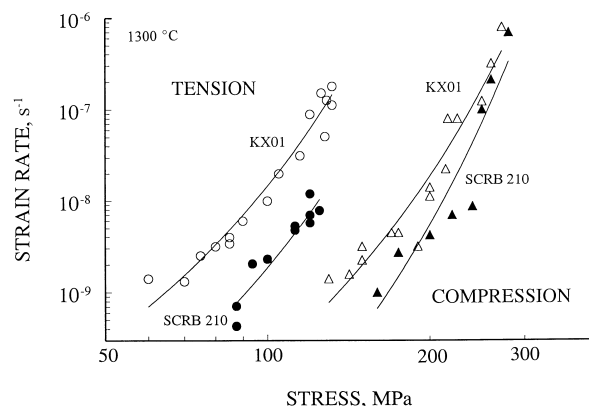


Fig. 7. Tensile and compressive creep behavior of SCRB210 and KX01. In both of these materials creep occurs more easily in tension than in compression. Equation 3 was fitted, as an empirical equation, to each of the four sets of data to determine the relative uncertainties. For the KX01, these were 0.14 in tension and 0.25 in compression. For the SCRB 210, these were 0.16 in tension and 0.39 in compression.

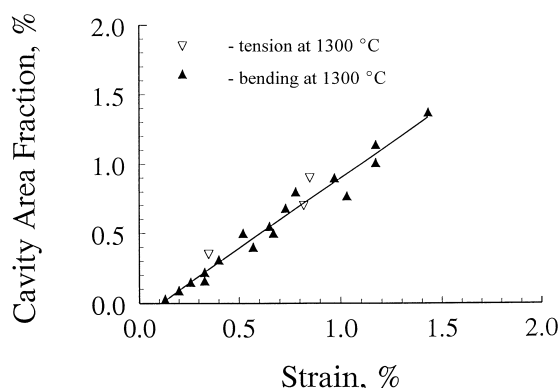


Fig. 8. Cavity formation in reaction-bonded silicon carbide, KX01. Volume fraction of cavities versus total strain.⁴⁶ For this linear fit to the data, the relative uncertainty was 0.07.

3.2 Silicon nitride

Based on recent investigations of the creep behavior of a number of grades of silicon nitride, these materials have the following characteristics: (a) for much of the range of applied stress, creep occurs faster in tension than in compression;^{48–56} (b) in contrast to the creep behavior of most metals, creep in tension is not a power function of the applied stress;^{49–51,57–59} (c) cavity formation accompanies creep in tension;^{50,51,60–62} (d) the volume fraction of cavities in tension is linearly proportional to the axial creep strain;^{41,50,51,58} (e) cavitation in compression is much less than that in tension.^{50,53}

Figure 9 is a log-log plot of the tensile and compressive creep rates of SN88 (NGK Insulator, Inc., Nagoya, Japan) as a function of applied stress.⁶³ The microstructure of this material is shown in Fig. 3. The creep data in compression fit a power law function of applied stress with a stress exponent of 0.96 ± 0.08 and an activation energy of $491 \pm 37 \text{ kJ mol}^{-1}$. Both the stress exponent and

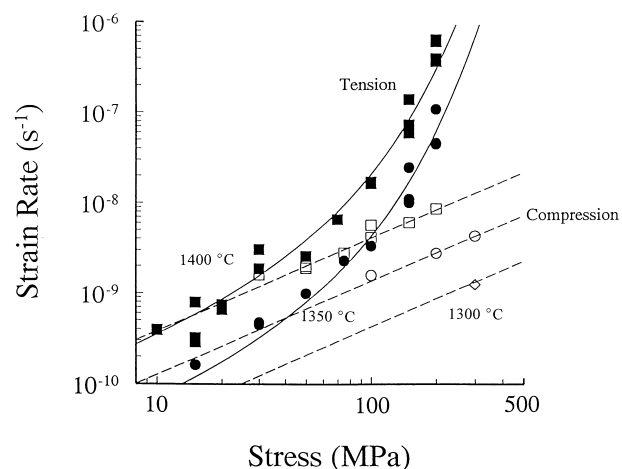


Fig. 9. Tensile and compressive creep rate of silicon nitride, SN88, as a function of applied stress. Compressive creep is given by the open symbols, tensile creep by the solid symbols: \square, \blacksquare 1400 °C; \circ, \bullet 1350 °C; \diamond 1300 °C.⁶⁴ Using eqn 3 the relative uncertainty for the compression data was 0.06. The relatively uncertainty for the tension data, 0.16, was determined from the larger set of data shown in Fig 12.

activation energy are within the range of values obtained in other studies of the compressive creep of silicon nitride.⁴² In tension, the creep data are curved over the entire range of the data. At low stresses, the tensile creep data approach a straight line with a slope of 1.

Microstructural examination of the gauge sections of crept specimens of many different grades of silicon nitride show that cavities form primarily at multi-grain junctions within pockets of the residual sintering aid.^{50,59,61–63} Examples of the kind of cavities that form in SN88 are shown in Fig. 10. The shapes of these cavities are the same as the silicate pockets in the undeformed material. Cavity growth involves the flow of the sintering aid away from the cavitation site, along triple junction channels to other silicate pockets in the microstructure. Simultaneously, a slight dilation of the structure occurs to accommodate the sintering aid previously located in the pocket. Similar creep asymmetry^{50,53,54} and nonlinear behavior^{50,51,58} on a log-log plot have also been observed on other grades of silicon nitride.

The relationship between the volume fraction of cavities and the total axial strain is shown in Fig. 11 for SN88.⁵⁹ Cavities form in tension at all applied stresses used in Fig. 9, even at stresses as low as 15 MPa. As with the KX01, the volume fraction of cavities increases linearly with the axial strain for each material tested. This linear relationship occurs in most silicon nitrides,^{50,51,58,63,64} usually with a slope close to unity.⁴⁹ For NT154, the volume fraction of cavities generated in compression was less than 10% of the volume fraction in tension,⁵⁰ suggesting that compressive stresses retard cavity formation.

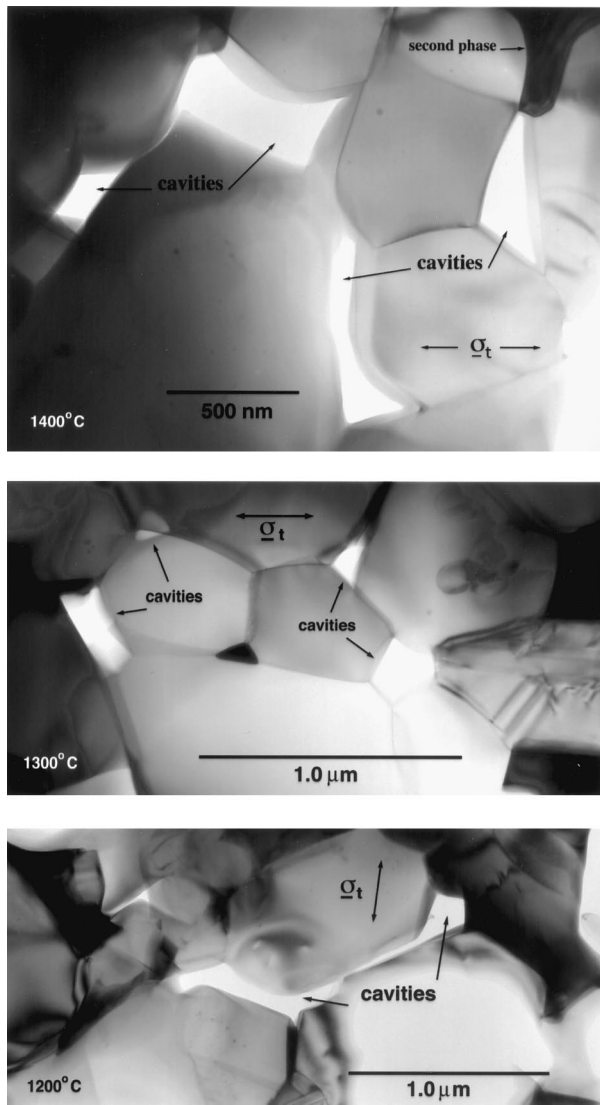


Fig. 10. Transmission electron micrograph of cavity formation in silicon nitride, SN88, which was subjected to a tensile stress. Cavities form within the silicate phase located at multi-grain junctions.

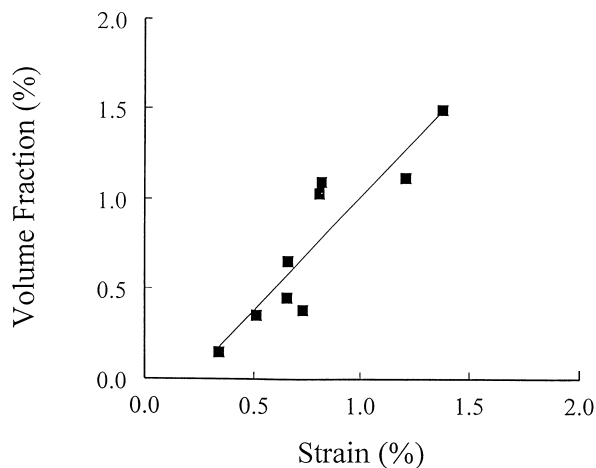


Fig. 11. The relationship between the volume fraction of cavities and total axial strain for SN88. The slope of the least square fitted line is close to 1.⁵⁹ The relative uncertainty of this data is 0.21.

4 Mechanisms of Creep

In this section of the paper, we first review classical theories of creep deformation that relate to materials with “dry” grain boundaries. Then we describe a new cavitation-based theory of deformation developed to rationalize the creep of materials with “wetted” boundaries such as silicon nitride.^{49,64} Means of improving creep resistance for both kinds of materials are then suggested.

4.1 Dislocation and diffusion mechanisms of creep

Classical mechanisms of creep deformation are based on the assumption that creep is a consequence of dislocation motion or diffusion.⁶⁵ Most theories suggest that the steady state creep rate, $\dot{\epsilon}_s$, should be a power function of the grain size, d , and applied stress, σ :

$$\dot{\epsilon}_s = \dot{\epsilon}_0 (\sigma/\sigma_0)^n (d/d_0)^m \exp\left(-\frac{\Delta H}{RT}\right) \quad (1)$$

The parameters, $\dot{\epsilon}_0$, n , m and ΔH , are empirical constants of the fit; ΔH is the apparent activation energy for creep. The magnitudes of the stress exponent, n , and the grain size exponent, m , depend on the mechanism of creep, as does ΔH . If creep can be described by a diffusional model,⁶⁶ then n should have a value of 1 or 2 and the parameter, m , should have a value of either -2 or -3 depending on whether diffusion occurs through the grains^{66,67} or along grain boundaries.⁶⁸ A dependence of a creep rate on $\exp(-1/\sigma)$ for a mechanism of diffusion creep has also been suggested by Wakai⁶⁹ for a solution precipitation mechanism that is interface rather than transport-controlled. For dislocation mechanisms, n is expected to have a value between 3 and 5, depending on the mechanism.⁶⁶ The grain size exponent, m , is expected to have a value of 0, i.e. the creep rate should not depend on grain size when dislocations are involved in the creep process.⁶⁶ A final consequence of diffusion or dislocation-controlled creep is the equality of the creep rate in tension and compression.

Compressive creep data on several grades of sintered or reaction bonded silicon carbide have been shown to be consistent with Eq. 1. As can be seen in Fig. 6, the compressive creep data can be represented by straight lines when plotting $\log \dot{\epsilon}_s$ versus $\frac{1}{RT}$, indicating an Arrhenius temperature behavior. The data on the compressive creep of Hexoloy can be fitted to two straight, suggesting a change in creep mechanism at about 1647°C. Also, when the compressive creep rates are plotted as a function of stress on logarithmic axes, they also fit straight lines indicating that the creep rate is a power function of

the applied stress. The stress exponents of the sintered grades of silicon carbide range from about 1.4 to 1.8. A number of creep mechanisms have been suggested for these materials. Above 1647°C, the creep of Hexoloy is believed to be the result of lattice diffusion accompanied by grain boundary sliding.¹² Below this temperature grain boundary diffusion accompanied by grain boundary sliding controls creep.¹² At stresses up to approximately 600 MPa, the creep behavior of SiC A and SiC B are both attributed to grain boundary diffusion accompanied by grain boundary sliding.⁴³ At higher stresses, the stress exponent increases to a value of 3.5–4 and dislocations play a dominant role in the creep process.⁴³ SiC B creeps about 2–5 times as fast as SiC A even though its grain size is about five times as large. This difference in creep rate is attributed to differences in impurity concentration between the two materials; the SiC A is made by hot pressing without sintering aids and hence is purer than SiC B.⁴³ The NC430 was tested above the melting point of silicon, 1414°C,⁷⁰ so that the creep is entirely due to deformation of the silicon carbide. The creep of this material is believed to be a consequence of dislocation climb.¹⁰ The excellent creep resistance of the silicon carbides shown in Fig. 6 is a consequence of the high temperatures required for diffusive transport in silicon carbide^{71,72} and the fact that dislocation glide is also difficult in this material.¹¹

Compressive creep behavior of liquid-phase sintered silicon nitride can also be described by Eq. 1. Several studies on this material show that the stress exponent lies between 1 and 2 for many grades of silicon nitride.^{49,73–78} Creep on this material is probably a consequence of solution precipitation, a diffusion process in which the liquid phase acts as a fast diffusion path for ion migration.^{79–82} Under a chemical potential gradient set up by the applied stress, silicon and nitrogen ions dissolve into the silicate phase at regions of high local stress. They then migrate through the grain boundary phase and precipitate onto the silicon nitride grains in regions where the local stresses are low. As noted by Pharr and Ashby,⁸² this process is the same as that occurring in Coble creep.⁸³

4.2 Mechanisms of creep that involve the formation of cavities

Cavitation in silicon nitride at multi-grain junctions involves the nucleation and growth of cavities within the silicate phase.⁵⁰ As the cavities grow, the silicate phase moves from the cavitated pockets to other silicate pockets in the material, either by diffusion or by mass flow. The distance over which the silicate phase moves during the formation of a cavity is equal to about one-half the distance

between active cavities.* Because the silicon nitride is fully dense before the silicate pockets cavitate, a slight dilation of the microstructure is required to make room for the silicate phase that was in the pockets.

In materials such as silicon nitride and siliconized silicon carbide (KX01), volume expansion caused by cavitation occurs primarily in the axial direction.^{49,63} Very little change in the lateral dimensions is observed during deformation. In modeling the deformation, Luecke and Wiederhorn^{49,65} therefore, assumed that all of the deformation occurring during creep is due to cavitation. They also assume that the net result of cavity formation is an increase in the length of the material, i.e. no change in lateral dimensions. By assuming that the flow of the silicate phase from the cavity is the rate limiting step for creep, they obtain the following equation for the creep rate, $\dot{\epsilon}_s$:

$$\dot{\epsilon}_s = \frac{\dot{\epsilon}_0}{\eta} \frac{V_f^3}{(1 - V_f)^2} \sigma \exp(\alpha\sigma) \quad (2)$$

where V_f is the volume fraction of second phase, σ is the applied stress and η is the effective viscosity of the silicate phase in the multi-grain pockets of the microstructure. The creep rate in Eq. 2 increases exponentially with the applied stress at high values of the stress and linearly with the applied stress at low values of the stress. Since V_f is normally small, the creep rate increases as V_f^3 . Also, because viscosity depends on temperature, $\eta \approx \eta_0 \exp(\frac{\Delta H}{RT})$, Eq. 2 may be represented in the following form:

$$\dot{\epsilon}_s = \frac{\dot{\epsilon}_0}{\eta_0} \frac{V_f^3}{(1 - V_f)^2} \sigma \exp(\alpha\sigma) \exp\left(-\frac{\Delta H}{RT}\right) \quad (3)$$

In Fig. 12, eqn 3 has been fitted to a set of tensile creep data collected on SN88.⁶⁴ The data set contains 58 data points on 41 test specimens. Equation 3 captures the stress and temperature dependence of this data very well. The equation also gives a good representation of the creep data for two other commercial grades of silicon nitride (NT154 and AS800).^{50,58}

Equation 3 predicts that the creep rate does not depend on the grain size. This prediction is hard to check as there have been few investigations of the variation of the creep rate with microstructural variables such as grain size. However, Haig *et al.*,^{84,85}

*Active cavities are the cavities that are in the process of forming. Once the pocket in which the cavity forms is completely drained of silicate phase, cavity growth stops.

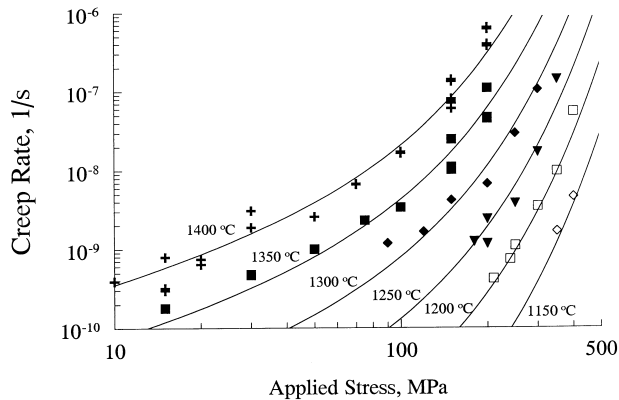


Fig. 12. A fit of eqn 3 to tensile data collected on SN88. The 58 data points in this figure were obtained from 41 tensile specimens.⁶⁴ The relative uncertainty for this data was 0.16.

in a study on two grades of silicon nitride with the same composition, but different grain size, showed that creep rate does not depend on grain size.* Unpublished studies by French *et al.*⁸⁶ also suggest little if any dependence of the creep rate on grain size, whereas unpublished studies by Luecke and Wallace⁸⁷ suggest a small increase in the creep rate with grain size. Flexural creep studies of various compositions of silicon nitride by Rendtel *et al.*⁸⁸ have shown a $1/d$ dependence of the creep rate on grain size. However, since the mechanism of creep in tension and compression may differ,⁴⁹ it is not clear how a grain size dependence of the creep rate in flexure relates to the grain size dependence in tension.

Understanding the dependence of the creep rate on grain size is problematic because of the difficulty in changing the grain size as the only microstructural variable. Usually, a given composition of silicon nitride is simply annealed in nitrogen to promote grain growth. However, this treatment can also affect other microstructural variables, such as the grain size distribution and the composition of the silicate phase. To get a clearer picture of just how the creep rate depends on one of these microstructural parameters, all of the other microstructural parameters important to the creep equation must be controlled as well. These include the volume fraction of silicate phase, the chemical composition of the silicate phase, and the grain size distribution. Control of these parameters to characterize creep behavior of glass-bonded ceramics has not been achieved to date in any systematic way.

4.3 Improving creep resistance of ceramics

In this paper, we have argued that two kinds of microstructures exist for high temperature structural ceramics: those in which the grains are directly

bonded via grain boundaries and those in which the grains are separated by a second phase. In directly bonded microstructures, classical mechanisms of deformation control the rate of creep. Deformation then involves dislocation motion or diffusive transport of material, either along grain boundaries, or through the grains. Diffusion plays an important role in the creep process by controlling the rate of climb of dislocations, or by changing the shape of the grains. Additives that increase the diffusion rate in the silicon carbide will also increase the creep rate. Therefore, one way to improve the creep resistance of these materials is to reduce the amount of sintering aid. This goal can also be achieved by avoiding the use of sintering aids entirely, as is done in NT230, where carbon is reacted with molten silicon to produce a highly creep resistant grade of silicon carbide, Fig. 5.

The main problem with silicon carbide, however, is not its creep resistance, which is better than that of most ceramic materials, but its low toughness, $K_{Ic} \approx 3 \text{ MPa} \cdot \text{m}^{1/2}$.⁸⁹ Some attempts have been made to increase the toughness of α -SiC by seeding it with β -SiC grains and by using additives that promote plate-like grain growth.^{90,91} This procedure produces a structure that is similar to that of liquid-phase sintered silicon nitride; it improves toughness to as high as $K_{Ic} \approx 9.5 \text{ MPa} \cdot \text{m}^{1/2}$.⁹¹ High-temperature creep of these materials has yet to be systematically studied. As in silicon nitride, we suspect that the low melting additives that might be used to achieve high toughness in silicon carbide would also limit its creep resistance at high temperatures.

Of the high-temperature ceramic materials that have a second phase at the grain boundary, the strongest and toughest is silicon nitride. Commercial grades of silicon nitride are available with mean tensile strengths ranging from 600 to 800 MPa⁴⁰ and toughness in the range $K_{Ic} \approx 6\text{--}8 \text{ MPa} \cdot \text{m}^{1/2}$.³⁸ Higher strengths and toughnesses have been obtained on experimental grades of the material.^{92,93} The best of the commercial compositions, however, cannot be used above 1400°C at stresses of 100 MPa because of the silicate phase at the grain boundaries, Fig. 5. At an equivalent stress and creep rate, this temperature is about 100 °C less than can be achieved with sintered silicon carbide. Liquid-phase sintered silicon nitride can be made more creep resistant by increasing the refractoriness of the silicate phase that bonds the silicon nitride grains together. This has been achieved on experimental billets containing only silica as a bonding phase,³⁸ or by using silica with a limited amount of Y_2O_3 as a sintering aid.^{31,94} However, a much lower fracture toughness was obtained for these materials, $2.5 \text{ MPa} \cdot \text{m}^{1/2}$.^{38,94}

*A preliminary study⁸⁴ indicated a slight decrease in creep rate with increasing grain size, but the final study,⁸⁵ which incorporated much more data, indicated no effect of grain size.

probably due to a stronger bond between the grains and the silicate phase and a blockier shape to the grains.⁹⁵ Sintering aids that yield tougher grades of silicon nitride,^{32–35} also degrade the creep resistance.⁴² Eliminating the grain boundary phase entirely, as is done in reaction-bonded silicon nitride, improves the creep resistance to that of sintered α -SiC,¹ but also decreases its toughness to a value of about $2.5 \text{ MPa} \cdot \text{m}^{1/2}$.¹ This observation is consistent with the findings of Hoffmann *et al.*⁹⁴ on experimental grades of silicon nitride. Thus, there is a problem in designing the microstructure of silicon nitride for high temperature creep resistance. Grades of silicon nitride that are more creep resistant are not as tough and *vice versa*. The development of a silicon nitride or silicon carbide that is both tough and creep resistant is a future challenge for material scientists.

5 Summary

This paper presents a review of the creep behavior of sintered α -SiC and liquid-phase sintered β -Si₃N₄. Sintered α -SiC has “dry” grain boundaries, i.e., the grain boundaries contain no second phase. Creep occurs by deformation of the grains themselves by either diffusion or dislocation motion. Consequently, sintered α -SiC is a creep resistant material that can be deformed easily only at temperatures greater than 1500°C . The creep resistance of α -SiC can be improved further by reaction bonding, which eliminates the use of the sintering aids that also enhance the creep rate. Because α -SiC has an equiaxed microstructure, it is weak, $\sigma_b < 500 \text{ MPa}$, and has a low toughness, $K_{Ic} = 2\text{--}4 \text{ MPa} \cdot \text{m}^{1/2}$. Higher toughness grades of SiC can be made by liquid-phase sintering, but this process has the potential of degrading the creep resistance of silicon carbide.

The toughness of silicon nitride is improved by using a silicate phase as a sintering aid. Such aids stimulate the growth of long grains that enhance the toughness of the ceramic. Accordingly, commercial grades of silicon nitride are now made with a toughness that ranges from about $K_{Ic} = 6\text{--}8 \text{ MPa} \cdot \text{m}^{1/2}$. A drawback to the silicate phases is their low melting point. When the grain boundaries are completely covered by the silicate phase, as they are in silicon nitride, the creep resistance is reduced. The best creep resistant grades of liquid-phase sintered silicon nitride are limited to a temperature of approximately 100°C less than that of sintered α -SiC. More creep resistant grades of silicon nitride can be made by reducing the amount of sintering aid or by using silica glass as a sintering aid, but then the toughness is low.

References

1. Richerson, D.W., *Modern Ceramic Engineering, Properties Processing, and Use in Design*, 2nd edn. Marcel Dekker, Inc., New York, 1992.
2. Dapkunas, S. J., Ceramic heat-exchangers. *Bull. Am. Ceram. Soc.*, 1988, **67**(2), 388–391.
3. For current work on automotive applications see *6th International Symposium on Ceramic Materials and Components for Engines*, ed. K. Niihara, S. Kanzaki, K. Komeya, S. Hirano and K. Morinaga. Japan Fine Ceramics Association, Halifax Onarimon Bldg. 6F, 3-24-10, Nishi-Shimbashi, Minatoku, Tokyo 105-0003, Japan, Printed by Technoplaza Co., Ltd., 1998.
4. Herbell, T. P. and Sanders, W. A., Monolithic ceramics. In *Flight-Vehicle Materials, Structure, and Dynamics, Assessment and Future Directions, Vol. 3: Ceramics and Ceramic-Matrix Composites*, ed. S. R. Levine. The American Society of Mechanical Engineers, New York, 1992, pp. 19–41.
5. Parthasarathy, V. M., Price, J. R., Brentnall, W. D., Graves, G. A. and Goodrich, S., Material characterization of candidate silicon based ceramics for stationary gas turbine applications. *ASME Paper 95-GT-249, ASME International Gas Turbine and Aeronautical Congress and Exposition*, Houston, TX, June, 1995.
6. Parthasarathy, V., van Roode, M., Price, J. and Gates, S., Review of Solar's ceramic stationary gas turbine development program. In *6th International Symposium on Ceramic Materials and Components for Engines*, ed. K. Niihara, S. Kanzaki, K. Komeya, S. Hirano and K. Morinaga. Japan Fine Ceramics Association, Halifax Onarimon Bldg. 6F, 3-24-10, Nishi-Shimbashi, Minatoku, Tokyo 105-0003, Japan, Printed by Technoplaza Co., Ltd., 1998, pp. 259–264.
7. Nakashima, T., Tatsumi, T., Takehara, I., Ichidawa, Y. and Kobayashi, H., Research and Development of CTGT 302. In *6th International Symposium on Ceramic Materials and Components for Engines*, ed. K. Niihara, S. Kanzaki, K. Komeya, S. Hirano and K. Morinaga. Japan Fine Ceramics Association, Halifax Onarimon Bldg. 6F, 3-24-10, Nishi-Shimbashi, Minatoku, Tokyo 105-0003, Japan, Printed by Technoplaza Co., Ltd., 1998, pp. 233–236.
8. Davis, R. F. and Carter, Jr. C. H., A review of creep in silicon nitride and silicon carbide. In *Advanced Ceramics*, Shinroku Saito, Oxford University Press, 1988, pp. 95–125.
9. Raj, R., Fundamental research in structural ceramics for service near 2000°C . *J. Am. Ceram. Soc.*, 1993, **76**(9), 2147–2174.
10. Carter, C. H. Jr. and Davis, R. F., Kinetics and mechanisms of high-temperature creep in silicon carbide: I, Reaction-bonded. *J. Am. Ceram. Soc.*, 1984, **67**(6), 409.
11. Carter, C. H. Jr. and Davis, R. F., Kinetics and mechanisms of high-temperature creep in silicon carbide: II, Chemically vapor deposited. *J. Am. Ceram. Soc.*, 1984, **67**(11), 732–740.
12. Lane, J. E., Carter, C. H. Jr. and Davis, R. F., Kinetics and mechanisms of high-temperature creep in silicon carbide: III, Sintered α -silicon carbide. *J. Am. Ceram. Soc.*, 1988, **71**(4), 281–295.
13. Prochazka, S. and Scanlan, R. M., Effect of boron and carbon on sintering of SiC. *J. Am. Ceram. Soc.*, 1975, **58**(1–2), 72.
14. Schlichting, J. and Riley, F. L., Silicon carbide. In *Concise Encyclopedia of Advanced Ceramic Materials*, ed. R. J. Brook. Pergamon Press, Oxford, 1991, pp. 426–429.
15. Prochazka, S., Sintering of silicon carbide. In *Ceramics for High Performance Applications*, ed. J. J. Burke, A. E. Gorum and R. N. Katz. Brook Hill Publishing Co, Chestnut Hill, MA, 1974, pp. 239–252.
16. Schlichting, J., Chemical vapour deposition of silicon carbide. *Powder Metall. Int.*, 1980, **12**, 141–147.

17. Riley, F. L., Silicon nitride. In *Concise encyclopedia of Advanced Ceramic Materials*, ed. R. J. Brook. Pergamon Press, Oxford, 1991, pp. 434–437.
18. Hockey, B. J. and Wiederhorn, S. M., Effect of microstructure on the creep of siliconized silicon carbide. *J. Am. Ceram. Soc.*, 1992, **75**(7), 1822–1830.
19. Clarke, D. R. and Thomas, G., Boundary phases in a hot-pressed MgO fluxed silicon nitride. *J. Am. Ceram. Soc.*, 1977, **60**(11–12), 491–495.
20. Lou, L. K. V., Mitchell, T. E. and Heuer, A. H., Impurity phases in hot-pressed Si_3N_4 . *J. Am. Ceram. Soc.*, 1978, **61**(9–10), 392–396.
21. Moulson, A. J., Reaction-bonded silicon nitride: its formation and properties. *J. Mater. Sci.*, 1979, **14**, 1017–1051.
22. Sawyer, G. R. and Page, T. F., Microstructural characterization of “REFEL” (reaction-bonded) silicon carbide. *J. Mater. Sci.*, 1978, **13**, 885–904.
23. Hockey, B. J. unpublished data.
24. French, J. D., Wiederhorn, S. M. and Yeckley, R. L., High temperature strength of a grade of siliconized-silicon carbide containing 8% volume fraction silicon, to be published.
25. Greskovich, C. D. and Rosolowski, J. H., Sintering of covalent solids. *J. Am. Ceram. Soc.*, 1976, **59**(7–8), 336–343.
26. Mitomo, M., Pressure sintering of silicon nitride. *J. Mater. Sci.*, 1976, **11**, 1103–1107.
27. Clarke, D. R., On the equilibrium thickness of intergranular glass phases in ceramic materials. *J. Am. Ceram. Soc.*, 1987, **70**(1), 15–22.
28. Kleebe, H.-J., Structure and chemistry of interfaces in Si_3N_4 ceramics studied by transmission electron microscopy. *J. Ceram. Soc. Jpn.*, 1997, **105**(6), 453–475.
29. Bonnell, D. A., Structure of grain boundary phases in silicon nitride. *Mater. Sci. Forum*, 1989, **47**, 132–142.
30. Falk, L. K. L. and Dunlop, G., Crystallization of the glassy phase in an Si_3N_4 material by post-sintering heat treatment. *J. Mater. Sci.*, 1987, **22**, 4369–4376.
31. Woetting, G. and Gugel, E., Influence of the grain-boundary phase amount on properties of dense Si_3N_4 . *CFI-Ceramic Forum International*, 1997, **74**(5), 239–244.
32. Pyzik, A. J., Carroll, D. F., Hwang, C. J. and Prunier, A. R., Self-reinforced silicon nitride—a new microengineered ceramic. In *The 4th International Symposium on Ceramic Materials and Components for Engines*, ed. R. Carlsson, T. Johansson and L. Kahlman. Elsevier Applied Science, London, 1992, pp. 584–593.
33. Pyzik, A. J. and Beaman, D. R., Microstructure and properties of self-reinforced silicon nitride. *J. Am. Ceram. Soc.*, 1993, **76**(11), 2737–2744.
34. Selkregg, K. R., More, K. L., Seshadri, S. G. and McMurty, C. H., Microstructural characterization of silicon nitride ceramics processed by pressureless sintering, overpressure sintering and sinter HIP. *Ceram. Eng. Sci. Proc.*, 1990, **11**(7–8), 603–615.
35. Wötting, G., Kanka, B. and Ziegler, G., Microstructural development, microstructural characterization and relation to mechanical properties of dense silicon nitride. In *Non-Oxide Technical and Engineering Ceramics*, ed. S. Hampshire. Elsevier, London, 1986, pp. 83–96.
36. Becher, P. F., Hwang, S.-L. and Hsueh, C.-H., Using microstructure to attack the brittle nature of silicon nitride ceramics. *MRS Bull.*, 1995, **20**(2), 23–27.
37. Becher, P. F., Microstructural design of toughened ceramics. *J. Am. Ceram. Soc.*, 1991, **74**(2), 255–269.
38. Pezzotti, G. and Sakai, M., Effect of silicon carbide “nano dispersion” on the mechanical properties of silicon nitride. *J. Am. Ceram. Soc.*, 1994, **77**(11), 3039–3041.
39. Woetting, G., Feuer, H., Frassek, L., Schoenfelder, L. and Leimer, G., Si_3N_4 materials: their properties and technical applications. *CFI-Ceram. Forum Int.*, 1998, **75**(7), 25–30.
40. Data Sheet SP-00244 on GS-44CL, GS-44SG and AS-800 from AlliedSignal Ceramic Components, Torrance, CA.
41. Krause, Jr., R. F., Luecke, W. E. and Wiederhorn, S. M., A comparison of tensile creep results on silicon nitride. *J. Am. Ceram. Soc.*, In review.
42. Luecke, W. E., Review: Creep of Si_3N_4 . In preparation.
43. Backhaus-Ricoult, M., Mozdierz, N. and Eveno, P., Impurities in silicon carbide ceramics and their role during high temperature creep. *J. Phys. III France*, 1993, **3**, 2189–2210.
44. Carroll, D. F. and Tressler, R. E., Accumulation of creep damage in a siliconized silicon carbide. *J. Am. Ceram. Soc.*, 1988, **71**(6), 472–477.
45. Fields, B. A. and Wiederhorn, S. M., Creep cavitation in a siliconized silicon carbide tested in tension and flexure. *J. Am. Ceram. Soc.*, 1996, **79**(4), 977–986.
46. Wiederhorn, S. M. and Hockey, B. J., High temperature degradation of structural composites. *Ceramics Int.*, 1991, **17**, 243–252.
47. Wiederhorn, S. M., Chuck, L., Fuller, E. R. and Tighe, N. J., Creep rupture of siliconized silicon carbide. In *Tailoring Multiphase and Composite Ceramics*, ed. R. E. Tressler, G. L. Messing, C. G. Pantano and R. E. Newnham, Plenum Publishing Corp., New York, 1986, pp. 755–773.
48. Luecke, W. E. and Wiederhorn, S. M., A new model for tensile creep of silicon nitride. *J. Am. Ceram. Soc.*, in press.
49. Luecke, W. E., Wiederhorn, S. M., Hockey, B. J., Krause, Jr. R. and Long, G. G., Cavitation contributes substantially to tensile creep in silicon nitride. *J. Am. Ceram. Soc.*, 1995, **78**(8), 2085–2096.
50. Gasdaska, C. J., Tensile creep in an *in situ* reinforced silicon nitride. *J. Am. Ceram. Soc.*, 1994, **77**(9), 2408–2418.
51. Kossowsky, R., Miller, D. G. and Diaz, E. S., Tensile and creep strengths of hot pressed Si_3N_4 . *J. Mater. Sci.*, 1975, **10**, 983–997.
52. Hockey, B. J., Wiederhorn, S. M., Liu, W., Baldoni, J. G. and Buljan, S.-T., Tensile creep of whisker-reinforced silicon nitride. *J. Mater. Sci.*, 1991, **26**, 3930–3931.
53. Ferber, M. K., Jenkins, M. G. and Tennery, V. J., Comparison of tension, compression, and flexure creep for alumina and silicon nitride ceramics. *Ceram. Eng. Sci. Proc.*, 1990, **11**(7), 1028–1045.
54. Liu, K. C., Stevens, C. O., Brinkman, C. R. and Holshauser, N. E., A technique to achieve uniform stress distribution in compressive creep testing of advanced ceramics at high temperatures. *J. Eng. Gas Turbines Power*, 1988, **119**, 500–505.
55. Wereszczak, A. A., Kirkland, T. P., Lin, H.-T. and Ferber, M. K., Tensile creep performance of a developmental, *in situ* reinforced silicon nitride. *Ceram. Eng. Sci. Proc.*, 1997, **18**(4), 45–55.
56. Lofaj, F., Usami, H., Okada, A. and Kawamoto, H., Long-term creep damage development in a self-reinforced silicon nitride. In *Engineering Ceramics '96: Higher Reliability through Processing*, ed. G. N. Babini *et al.*, Kluwer Academic Publishers, 1997, pp. 337–352.
57. Maupas, H., Hockey, B. J. and Wiederhorn, S. M., Tensile creep of a commercial-grade of silicon nitride: limitation of Norton's relationship? To be published.
58. Krause, Jr., R. F., Luecke, W. E., French, J. D., Hockey, J. and Wiederhorn, S. M., Tensile creep and rupture of silicon nitride. *J. Am. Ceram. Soc.*, 1999, **82**(5), 1233–1241.
59. Gürtler M. and Grathwohl, G., Tensile creep testing of sintered silicon nitride. In *Proceedings of the Fourth International Conference on Creep and Fracture of Engineering Materials and Structures*, Institute of Metals, London, 1990, pp. 399–408.
60. Menon, M. N., Fang, H. T., Wu, D. C., Jenkins, M. G., Ferber, M. K., More, K. L., Hubbard, C. R. and Nolan, T. A., Creep and stress rupture behavior of an advanced silicon nitride: Part I—experimental observations. *J. Am. Ceram. Soc.*, 1994, **77**(5), 1217–1227.
61. Ohji, T. and Yamauchi, Y., Tensile creep and creep rupture behavior of monolithic and SiC whisker-reinforced silicon nitride ceramics. *J. Am. Ceram. Soc.*, 1993, **76**, 3105–3112.

62. Lofaj, F., Okada, A. and Kawamoto, H., Cavitation strain contribution to tensile creep in vitreous bonded ceramics. *J. Am. Ceram. Soc.*, 1997, **80**(6), 1619–1623.
63. Yoon, K. J., Wiederhorn S. M. and Luecke, W. E., A comparison of tensile and compressive creep behavior in silicon nitride. *J. Am. Ceram. Soc.*, in review.
64. Wiederhorn, S. M. and Luecke, W. E., Creep of silicon nitride. In *Computer Aided Design of High Temperature Materials*, ed. A. Pechenik, R. K. Kalia and P. Vashishta. Oxford University Press, Oxford, to be published.
65. Poirier, J.-P., *Creep of Crystals*. Cambridge University Press, Cambridge, England, 1995.
66. Nabarro, F. R. N., Deformation of crystals by the motion of single ions. *Report of a Conference on Strength of Solids (Bristol)*, The Physical Soc., 1948, pp. 75–90.
67. Herring, C., Diffusional viscosity of a polycrystalline solid. *J. Appl. Phys.*, 1950, **21**, 437–445.
68. Coble, R. L., A model for boundary diffusion controlled creep in ceramic materials. *J. Appl. Phys.*, 1963, **34**, 1679–1682.
69. Wakai, F., Step model of solution-precipitation creep. *Acta Metall. Mater.*, 1994, **42**, 1163–1614.
70. *CRC Handbook of Chemistry and Physics*, 79th edn. ed. D. R. Lide. CRC Press, Inc., W. Palm Beach, FL, 1998, pp. 4–82.
71. Hong, J. D. and Davis, R. F., Self-diffusion of carbon-14 in high purity and N-doped α -SiC single crystals. *J. Am. Ceram. Soc.*, 1980, **63**(9–10), 546–552.
72. Hong, J. D., Newberry, D. E. and Davis, R. R., Self-diffusion of ^{30}Si in α -SiC single crystals. *J. Mater. Sci.*, 1981, **16**(12), 2485–2494.
73. Lange, F. F., Davis, B. I. and Clarke, D. R., Compressive creep of $\text{Si}_3\text{N}_4/\text{MgO}$ alloys, Part 1, effect of composition. *J. Mater. Sci.*, 1980, **15**, 601–610.
74. Crampon, J., Duclos, R., Peni, F., Guicciardi, S. and De Portu, G., Compressive creep and creep failure of $8\text{Y}_2\text{O}_3/3\text{Al}_2\text{O}_3$ -doped hot-pressed silicon nitride. *J. Am. Ceram. Soc.*, 1997, **80**(1), 85–91.
75. Da Silva, C. and Davis, T. J., Compressive creep of silicon nitride. In *Creep and Fracture of Engineering Materials and Structures*, ed. B. Wilshire and R. W. Evans. The Institute of Metals, London, 1990, pp. 365–375.
76. Lange, F. F. and Davis, B. I., Compressive creep of $\text{Si}_3\text{N}_4/\text{MgO}$ alloys. *J. Mater. Sci.*, 1982, **17**, 3637–3640.
77. Birch, J. M. and Wilshire, B., The compression creep behaviour of silicon nitride ceramics. *J. Mater. Sci.*, 1978, **13**, 2627–2636.
78. Crampon, J., Duclos, R. and Rakotoharisoa, N., Compression creep of $\text{Si}_3\text{N}_4/\text{MgAl}_2\text{O}_4$ alloys. *J. Mater. Sci.*, 1990, **25**, 1203–1208.
79. Durney, D. W., Solution-transfer, an important geological deformation mechanism. *Nature*, 1972, **253**, 315–317.
80. Rutter, E. H., The kinetics of rock deformation by pressure solution. *Phil. Trans. Roy. Soc. Lond. A.*, 1976, **283**, 203–209.
81. Raj, R. and Chyung, C. K., Solution-precipitation creep in glass ceramics. *Acta metall.*, 1981, **29**, 159–166.
82. Pharr, G. M. and Ashby, M. F., On creep enhanced by a liquid phase. *Acta metall.*, 1983, **31**, 129–138.
83. Coble, R. L., A model for boundary diffusion controlled creep in ceramic materials. *J. Appl. Phys.*, 1963, **34**, 1679–1682.
84. Haig, S., Cannon, W. R. and Whalen, P. J., Anelastic recovery in crept silicon nitride. *Ceram. Eng. Sci. Proc.*, 1992, **13**(9–10), 1008–1023.
85. Haig, S. and Cannon, W. R., Tensile creep, recovery, and failure of an *in situ* reinforced silicon nitride. *J. Am. Ceram. Soc.*, in review.
86. French, J. D., Wiederhorn, S. M. and Hoffmann, M. J., Grain size effects on creep of silicon nitride. Unpublished research, 1997.
87. Luecke, W. E. and Wallace, J. S., Grain-size effects on tensile creep of silicon nitride. Unpublished research, 1997.
88. Rendtel, A., Hübner, H., Herrmann, M. and Schubert, C., Silicon nitride/silicon carbide nanocomposite materials: II, hot strength, creep, and oxidation resistance. *J. Am. Ceram. Soc.*, 1998, **81**(5), 1109–1120.
89. Tracy, C. A. and Quinn, G. D., Fracture toughness by the surface crack in flexure (SCF) method. *Ceram. Eng. and Sci. Proc.*, 1994, **15**, 837–845.
90. Padture, N. P., *In situ*-toughened silicon carbide. *J. Am. Ceram. Soc.*, 1994, **77**(2), 519–523.
91. Cao, J. J., Moberlay-Chan, W. J., DeJonghe, L. C., Gilbert, C. J. and Ritchie, R. O., *In situ* toughened silicon carbide with Al-B-C Additions. *J. Am. Ceram. Soc.*, 1996, **79**(2), 461–469.
92. Becher, P. F., Sun, W. Y., Plucknett, K. P., Alexander, K. B., Hueh, C.-H., Lin, H.-T., Waters, S. B., Westmoreland, C. G., Kang, E.-S., Hirao, K. and Breto, M. E., Microstructural design of silicon nitride with improved fracture toughness, Part I: effect of grain shape and size. *J. Am. Ceram. Soc.*, 1998, **81**(11), 2821–2830.
93. Kanzaki, S., Hirao, K., Brito, M. E., Watari, K., Toriyama, M., Imamura, H. and Kitayama, M., Development of high performance Si_3N_4 through textured microstructure control. Presented at 100th Annual Meeting of the American Ceramic Society, May 3–6, 1998.
94. Hoffmann, M. J., Geyer, A. and Oberacker, R., Potential of the sinter-HIP-technique for the development of high-temperature resistant Si_3N_4 -ceramics. *J. Eur. Ceram. Soc.*, 1999, **19**(13–14), this issue.
95. Pezzotti, G., Ota, K. and Kleebe, H.-J., Grain-boundary relaxation in high-purity silicon nitride. *J. Am. Ceram. Soc.*, 1996, **79**(9), 2237–2346.